

Molecular BioSystems

Accepted Manuscript



This is an *Accepted Manuscript*, which has been through the Royal Society of Chemistry peer review process and has been accepted for publication.

Accepted Manuscripts are published online shortly after acceptance, before technical editing, formatting and proof reading. Using this free service, authors can make their results available to the community, in citable form, before we publish the edited article. We will replace this *Accepted Manuscript* with the edited and formatted *Advance Article* as soon as it is available.

You can find more information about *Accepted Manuscripts* in the [Information for Authors](#).

Please note that technical editing may introduce minor changes to the text and/or graphics, which may alter content. The journal's standard [Terms & Conditions](#) and the [Ethical guidelines](#) still apply. In no event shall the Royal Society of Chemistry be held responsible for any errors or omissions in this *Accepted Manuscript* or any consequences arising from the use of any information it contains.



www.rsc.org/molecularbiosystems

**Metabonomic analysis of the therapeutic effect of *Potentilla discolor*
in treatment of Type 2 diabetes mellitus**

Yi Li^{ab1}, Jing-jing Li^{ab1}, Xiao-dong Wen^a, Rong Pan^c, Jie Yang^{ab*}

a State Key Laboratory of Natural Medicines, China Pharmaceutical University,
Nanjing, 210009, China

b Department of Chinese Materia Medica Analysis, China Pharmaceutical University,
Nanjing 210009, People's Republic of China

c AustarPharma LLC, 18 Mayfield Ave, Edison, NJ 08837, USA

¹Yi Li and Jing-jing Li contributed equally to this work.

*Correspondence to: Dr. Jie Yang, State Key Laboratory of Natural Medicines, China
Pharmaceutical University, Nanjing. E-mail: cpusyj@163.com

Abstract

Type 2 diabetes mellitus (T2DM) is increased worldwide in parallel with the obesity epidemic. *Potentilla discolor* is one of the most important crude materials in Traditional Chinese medicine (TCM) for therapy of hyperglycemia and hyperlipidemia. In this work, a plasma metabolomic approach based on the combination of UPLC-Q-TOF with multivariate data analysis was applied to investigate the therapeutic effects of extract of *P. discolor* (EPD) and corosolic acid (CA), a main bioactive compounds of *P. discolor*. Male C57BL/6 mice were fed with high-fat diet (HFD-fed group) for 8 weeks and then treated with EPD (EPD-treated group) or CA (CA-treated group) for another 8 weeks. After the experimental period, samples of plasma were collected and analyzed by ultra-performance liquid chromatography/quadrupole time of flight mass spectrometry (UPLC-Q-TOF). The principal components analysis (PCA) and partial least squares discriminant analysis (PLS-DA) models were built to find biomarkers of T2DM and investigate the therapeutic effects of EPD and CA. 26 metabolites, which are distributed in several metabolic pathways were identified as potential biomarkers of T2DM. Taken these biomarkers as screening indexes, EPD and CA could reverse the pathological process of T2DM through regulating the disturbed pathway of metabolism. The metabolomic results benefit not only for the evaluation of the therapeutic effect of TCM but also for the elucidation of the underlying molecular mechanism.

Keywords: T2DM; UPLC-Q-TOF; *Potentilla discolor*; corosolic acid; metabolomics;

Introduction

Type 2 diabetes mellitus (T2DM), increased worldwide in parallel with the obesity epidemic, has become a major challenge to the healthcare systems. Currently, 382 million people suffer from diabetes and the prevalence is expected to grow to 592 million by 2035 ¹. T2DM is characterized by a combination of insulin resistance, impaired hepatic gluconeogenesis, and altered β -cell function ². A number of therapeutic agents exist for the treatment of type 2 diabetes mellitus (T2DM), including metformin, sulfonylureas, DPP-4 inhibitors, PPAR γ agonists, α -glucosidase inhibitors, insulin, and GLP-1 analogs. However, in addition to inadequate efficacy and durability, some of these agents suffer from liabilities, including hypoglycemia, weight gain, edema, fractures, lactic acidosis, and gastrointestinal intolerance ³. Thus, there is an increasing need to search for high-effective and safety agents that would ameliorate T2DM.

Nowadays, herbal supplements have been applied for the treatment of T2DM worldwide. Of all the herbal medications used in T2DM, *Potentilla discolor* is one of the most important crude materials in Traditional Chinese medicine (TCM) for therapy of hyperglycemia and hyperlipidemia ⁴. Extract of *P. discolor* (EPD) was prepared with water, milk, and alcoholic solutions to treat T2DM in clinical research ⁵. Our previous studies also confirmed that EPD has hypoglycemic activity on alloxan-induced diabetic mice ⁶ and streptozotocin-induced diabetic rats ⁷. Though many pharmacological researches have been carried out to study the effect of *P. discolor* on T2DM ⁶⁻⁸, it remains a difficult task to clarify its mechanism due to the complexity of active compounds and their synergistic actions on multi-targets.

Metabolomics, as one of the core disciplines in the systems biology, can be expected to provide new insights into the global effects of the disease related to metabolic pathways ⁹. It reveals the whole metabolic changes profiles though monitoring entire pattern of low molecular weight compounds in body fluids rather than focusing on individual metabolites, reflecting the terminal symptoms of metabolic network of biological systems in holistic context ¹⁰. Therefore, it is a

potential tool for us to study the underlying efficacies and therapeutic mechanisms of TCM. Furthermore, the development of T2DM is highly correlated with uptake of the high fat diet. This could result in a number of metabolic perturbations including imbalance of glucose metabolism and dyslipidemia in key organs and blood plasma. Thus, metabolomics, aimed at measuring global metabolism changes would provide a good description of the phenotype of T2DM.

In this work, a plasma metabonomic approach based on the combination of UPLC-Q-TOF with multivariate data analysis was applied for the discovery of T2DM biomarkers. Furthermore, as corosolic acid (CA), one of the main compounds in EPD, has significant anti-diabetic activity, the metabonomic strategy was used for investigating the therapeutic effects of EPD and CA.

Materials and methods

Chemicals and Reagents

Acetonitrile and formic acid (HPLC grade) were obtained from ROE Scientific Inc. (Newcastle, USA). Methanol (HPLC grade) was purchased from Jiangsu Hanbon Sci. & Tech. Co. Ltd (Nanjing, China). Purified water (18.2M Ω -cm) prepared by the Millipore system (Millipore, Bedford, MA, USA) was used for all the preparations. Other reagents were of analytical grade. Leuchine enkephalin was purchased from Sigma. L-tryptophan and phenylalanine were obtained from Solarbio (Shanghai, China). Xanthosine was purchased from FeiYu Biological Technology (Nantong, China).

The kits for measurement of triglyceride (TG), total cholesterol (TC), fasting blood glucose (FBG), low density lipoprotein-cholesterol (LDL-c) and high density lipoprotein-cholesterol (HDL-c) were purchased from Jiancheng Bioengineering Institute (Nanjing, China). The mouse insulin ELISA kit was bought from Millipore.

Plant material and preparation of EPD

P. discolor was collected in November 2008 from natural habitat in Guangxi, China,

and authenticated by Professor Qiang Wang, Department of Chinese Materia Medica Analysis, China Pharmaceutical University, Nanjing, where a voucher specimen has been deposited (No. 20081201).

The crushed herb of *P. discolor* (2 kg) was extracted with 90% ethanol for three times (5 L each time) at room temperature (25 °C). Solutions were combined and concentrated under reduced pressure at 65 °C to yield the extract, and then distilled water was added to the extract. After being defatted with petroleum ether, the aqueous layer was partitioned with ethyl acetate. The ethyl acetate fraction was concentrated under vacuum to give 67 g powder and was used as the extract of *P. discolor*. The contents of CA in the extract were 3.4 %, determined by the HPLC-DAD method reported by Yang et al ¹¹.

Animals

Male C57BL/6 mice at 4 weeks of age were purchased from the Animal center of Yangzhou University (Yangzhou, Jiangsu, China). Three mice were placed in one cage, and maintained under controlled room temperature (20±2°C) and humidity (60-70%) with day /night cycle (12h/12h). All animals had free access to food and water. The animal care and study protocols were maintained in accordance with the Provisions and General Recommendation of Chinese Experimental Animals Administration Legislation. (Approved by the people's government of Jiangsu province on August 19, 2008 and promulgated by Decree No. 45 of the people's government of Jiangsu province)

Animal handling and sample collecting

The experimental protocol was shown in figure 1. After acclimatization for 5 days, the mice were fed with normal diet (10% kcal fat, 70% kcal carbohydrates, 20% kcal proteins) or high fat diet (HFD) (60% kcal fat, 20% kcal carbohydrates, 20% kcal proteins) for 8 weeks. The HFD-fed mice were randomized into HFD-fed group (n=6), EPD-treated group (n=6) and CA-treated group (n=6). The HFD-fed group and normal group were given high fat diet and normal diet respectively as before while the

EPD-treated group and CA-treated group were switched to HFD supplemented with EPD and CA (0.5%w/w, 0.017%w/w) respectively for 8 weeks. At the end of experiment, retro-orbital bleeding was conducted after overnight fasting for testing the plasma level of TG, TC, LDL-c, HDL-c, Insulin and FBG. Besides, the insulin resistance index [HOMA-IR= (FBG×Insulin)/22.5, homeostasis model assessment for insulin resistance] was calculated. In addition, body weight of the mice was taken on a weekly basis.

Glucose tolerance test

After treatment with EPD and CA for seven weeks, the mice were fasted for 6h and orally administrated of glucose (2g/kg body weight). The levels of tail venous blood glucose in individual mice were measured at 0, 30, 60 and 120 min post glucose challenge using test strips on an One Touch profile glucose Meter (Johnson & Johnson, New Brunswick, USA). The area under the curve (AUC) for the levels of blood glucose over the Experimental period was calculated.

Sample preparation

For UPLC-MS analysis, 300 μ L of methanol was added to 100 μ L aliquots of plasma. The mixture was vortex-mixed vigorously for 2 min and subsequently centrifuged at 14,000g for 10 min at 4 °C. The supernatant was transferred to autosampler vial kept and an aliquot of 4 μ L was injected for UPLC-MS analysis.

To examine the stability of LC-MS system, 150 μ L from each plasma sample was pooled to generate a pooled quality control (QC) sample and aliquots of 100 μ L of this pooled sample were extracted by the same method. Moreover, the QC sample was divided into six parts and extracted by the same method. These six samples were continuously injected to validate the repeatability of the sample preparation method.

UPLC-Q-TOF-MS conditions

The UPLC-MS analysis was performed on a 1290 Infinity UPLC system coupled with a 6530 UHD Accurate-Mass Q-TOF /MS (Agilent Technologies, USA).

Chromatographic separations were performed on a UPLC C₁₈ column (100 mm × 2.1 mm, 1.8 μm, Agilent) maintained at 40 °C. The mobile phase consisted of 0.1% formic acid (A) and ACN modified with 0.1% formic acid (B). The following gradient program was used: 5% B at 0-2 min, 5%-95% B at 2-17 min, 95% B at 17-19 min and followed by re-equilibrated step of 3 min. The flow rate was 0.4 mL/min and the injection volume was 4 μL.

An electrospray ionization source (ESI) interface was used and set in both positive and negative modes. The following parameters were employed: desolvation gas, 600L/h; cone gas, 50L/h; desolvation temperature, 350; source temperature, 100; capillary voltage, 4000V; Sampling cone, 35kV; extraction cone, 4V for positive mode. desolvation gas, 700L/h; cone gas, 50L/h; desolvation temperature, 300; source temperature, 100; capillary voltage, 3500V; Sampling cone, 50kV; extraction cone, 4V for negative mode. Collision energy was set at 15 or 30 eV in MS/MS mode for identification of potential biomarkers. Leucine enkephalin was used as the lock mass (*m/z* 556.2771 in the positive mode, and 554.2615 in the negative mode) to ensure the accuracy and reproducibility. The mass range was set at *m/z* 50-1000.

Data processing

The LC-MS data were exported by MassHunter and MassProlifer softwares (Agilent Corporation, MA, USA). Before multivariate analysis, the data of each sample was normalized to the total ion intensity per chromatogram. The principal components analysis (PCA) and partial least squares discriminant analysis (PLS-DA) was performed by the SIMCA-P 11.5 version (Umetrics AB, Umea, Sweden). The significance was expressed by using one-way analyses of variance (ANOVAs) of the SPSS 13.0 for Windows (SPSS Inc., Chicago, USA). *P* values less than 0.05 were considered significant.

Results

Effects of EPD and CA on body weights and plasma parameters in HFD-fed mice

In present study, C57BL/6 mice were fed with HFD or normal diet for 16 weeks. As shown in table 1, the body weights in the HFD groups were significantly greater than those of the normal group ($p < 0.01$). Furthermore, the levels of FBG and fasting plasma insulin in HFD group were near 2.01 and 5.20 times of normal group, respectively. The HOMA-IR of mice increased from 4.41 in the normal group to 46.27 in the HFD-fed group, suggesting that insulin resistance has been caused by HFD. Meanwhile, plasma levels of TG and TC in HFD-fed mice up-regulated significantly ($P < 0.01$) in comparison with those in normal group. In addition, the glucose tolerance test confirmed insulin resistance has been developed in HFD-fed mice (Figure 2). These indexes were similar to physiopathological state of type 2 diabetes, indicating the HFD-fed group has developed T2DM.¹²

By contrast, administration with EPD and CA could effectively improve these symptoms, as demonstrated by the markedly decrease in body weight (by 23.6% and 18.8%; $p < 0.01$), FBG (by 39.2% and 44.2%; $p < 0.01$), fasting plasma insulin and HOMA-IR (by 79.9% and 79.6%, by 87.8% and 88.6%; $p < 0.01$) compared with the HFD-fed group (Table 1). Besides, compared with HFD-fed mice, concentrations of plasma lipids, including TG and TC, significantly decreased after EPD and CA administration (Table 1). Meanwhile, the glucose tolerance test (Figure 2) revealed the values of AUC for blood glucose in the EPD and CA treated group were obviously lower than those in the HFD-fed group. Collectively, these data clearly indicated that treatment with EPD and CA significantly reduced the body weights, corrected hyperglycemia and glucose intolerance, and mitigated the HFD-induced hyperinsulinemia in HFD-fed mice.

LC-Q-TOF method validation

Three common ions in positive ion mode and in negative ion mode were selected for method validation, respectively. System stability was evaluated by analysis of a QC sample seven times at the beginning of the batch and then after every three samples. The relative standard derivations (RSDs) of these peaks were 5.67-12.84% for peak areas and 0.02-0.85% for retention times in the positive mode (5.88-11.83% for peak

areas and 0.01-0.76% for retention times in the negative mode). The data were listed in Table S1 in supplementary information.

Extracts from six aliquots of QC sample were continuously injected to evaluate the repeatability. A stable retention time for these selected ions was observed with RSD less than 0.81% in positive mode and 0.69% in negative mode. In addition, the RSD values for peak areas were varied from 7.89% to 12.15% in positive mode and from 6.86% to 13.07% in negative mode. The data were listed in Table S1 in supplementary information.

All the data indicated that the established sample analysis method is highly repeatable and stable, and could be used for analyzing large-scale samples in metabolomic experiments.

Plasma metabolite profile in HFD-fed mice and Identification of biomarkers

Typical LC-MS total ion current (TIC) chromatograms of a plasma sample in positive mode and negative mode are shown in Figure 3 and Figure S1. 1694 ions, including both positive and negative mode were obtained. Due to the large number of signals, multivariate data analysis was applied to reveal the metabolic changes in T2DM. Initially, principal components analysis (PCA), an unsupervised chemometric model, was carried out to explore correlations between normal and HFD-fed group. Complete separation between the HFD-fed group and normal group was observed in score plot from PCA ($R^2X=0.807$, $Q^2=0.61$ in positive mode and $R^2X=0.813$, $Q^2=0.481$ in negative mode)(Figure 4), indicating that metabolic profiles significantly changed in HFD-fed group.

Furthermore, a supervised partial least squares discriminant analysis (PLS-DA) technique was implemented to search distinct metabolites between normal and HFD-fed groups (Figure 5). The parameter R^2Y (0.999 in positive ion mode; 0.987 in negative ion mode) indicated that the established model was capable of differentiating normal group from HFD-fed group. The parameter Q^2 (0.997 in positive ion mode; 0.941 in negative ion mode) showed that the established model owned strong predictability. The S-plot (Figure 6) represents the impact of metabolites on the

clustering results. Variables that significantly contributed to the clustering were chosen according to a threshold of the variable importance in the projection (VIP>1). Then, these differential metabolites were validated using Student's t-test. The critical p-value was set to 0.05 for significantly differential variables in this study. Following the criterion above, a total of 76 variables contributed to the classification of these two groups. Among these perturbed variables, 26 variables (10 in positive mode and 16 in negative mode) were predicted by comparing the accurate MS and MS/MS fragments with the metabolites searching in databases (<http://metlin.scripps.edu>, <http://www.hmdb.ca/>), and then 3 of them were confirmed by the commercial standards. The identification results were listed in [Table S2](#).

Here, we take xanthosine (m/z 283.0669 in negative mode) as an example to illustrate the process of biomarker identification. Its MS/MS spectra are shown in Fig.7. First the quasi-molecular ion was found out to be a mass peak at m/z 283.0669 (retention time was 1.22 min in negative mode). $C_{10}H_{12}N_4O_6$ was calculated as the most probable molecule formula, and MS/MS information was used to study its molecular structure. The above information was also searched for in internet databases. Then, considering the elemental composition, fragmentation pattern, and chromatographic retention behavior, the m/z of 151.0251 was thought to be probably xanthosine. This was the confirmed by comparing with commercial standard.

Among those 26 identified biomarkers, 19 were increased in the plasma of HFD-fed mice while 7 were decreased compared with normal mice. ([Table S2](#))

Effects of EPD and CA on T2DM based on metabolite profile

The therapeutic effects of EPD and CA on the treatment of T2DM can be demonstrated not only from pharmacological experiments but also can be showed in metabolomic study. PCA was applied for investigating the therapeutic effects of EPD and CA by PCA.

The R2X and Q2 were 0.85 and 0.68 in positive mode and 0.83 and 0.57 in negative mode, which indicated the classifications were well for PCA models. The score plots (Figure 8) of the first two principal components allowed visualization of

the data and comparing of the four groups. The normal, HFD-fed, EPD and CA treatment groups are classified clearly. In addition, the EPD and CA-treatment groups are also classified clearly, indicating there are some different in the mechanisms of their therapeutic effects on T2DM.

To further evaluate the reversed condition of the potential biomarkers by administration of EPD and CA, the relative peak areas of the 26 metabolites to their respective total integrated area of the spectra were investigated (Figure 9). Compared to the HFD-fed group, all these metabolites were significantly reversed in EPD-treated group while 22 metabolites were also reversed in CA-treated group, demonstrating that EPD and CA had extensive effects in the treatment of T2MD through partially regulating the disturbed pathways of metabolism.

Discussion

P. discolor with long history of use in China has been proven to be effective in treating T2DM. Nevertheless, its activity evaluation and mechanistic understanding are still lacking. According to the chemical and pharmacokinetic analysis of EPD, we found that CA is a major component from EPD^{11, 13}. In addition to its content, it exhibits significant anti-hyperlipidemic, anti-oxidant and anti-inflammatory activities^{14, 15}. Therefore, in this work, a UPLC-Q-TOF based on metabolomic strategy was applied to study the plasma metabolic profile associated with T2DM and then investigate the therapeutic effects of EPD and CA on T2DM.

In this study, 26 identified biomarkers were identified by LC-Q-TOF. The related pathway of each biomarker was recorded in **Table S2** by searching the KEGG PATHWAY Database (<http://www.genome.jp/kegg/>). By relating the metabolic pathways, the metabolic network of the potential biomarkers was established and shown in Figure 10. As shown in Figure 10, we found that most pathways of the potential biomarkers were related to energy metabolism, including the lipid metabolism, amino acid metabolism and nucleotide metabolism.

Lipid metabolism

In all the 26 potential biomarkers, 5 biomarkers were related to glycerolphospholipid metabolism, suggesting this pathway altered a lot in HFD-fed group. Lysophosphatidylcholine (LPC) are produced as the result of PCs hydrolysis by phospholipase A2 (PLA2)¹⁶. High ambient glucose concentration in diabetes could activate protein kinase C (PKC), resulting the activation of PLA2¹⁷⁻¹⁹. With the development of T2DM, the PLA2 was activated and caused the hydrolysis of PCs to elevate plasma concentrations of LPCs. Both EPD and CA could reverse the changes in glycerolphospholipid metabolism. It has been reported LPCs could inhibit the phosphorylation of AKT²⁰. Thus, the PKB/AKT pathway that controls ultimately gluconeogenesis and glycogenolysis is severely affected which leads to hyperlycaemia and compensatory hyperinsulinaemia²¹. As EPD and CA could reduce the levels of LPCs, their therapeutic mechanism on T2DM might be partly related the PKB/AKT pathway.

Amino acid metabolism

Tryptophan was one of the biomarkers found in the plasma in our work. Its content was significantly reduced in T2DM and elevated to normal level after EPD treated. The increase of tryptophan after EPD treated might increase the level of 5-HT²², which might result in a suppressing in appetite²³ and thus contribute to the loss of weight. Meanwhile, N-Methyltryptamine, a metabolite of L-tryptophan decreased in HFD-fed group and return back after EPD treated, which may further predict EPD could regulate the L-tryptophan metabolism.

The levels of phenylalanine and its two metabolites (2-phenylacetamide and phenylglyoxylic acid) were up-regulated in T2DM in our study. It has been reported that the content of phenylalanine in plasma was positively correlated with leptin, a key hormone in regulating energy intake²⁴. Hyperleptinemia causes an increase in oxidative stress leading to the impairments of glucose uptake in muscle and fat²⁵. According to our data, the levels of phenylalanine and its two metabolites were reduced after treating EPD and CA, revealing EPD and CA might decrease the level

of leptin and alleviate oxidative stress in treating T2DM.

Nucleotide metabolism

The concentrations of hypoxanthine and xanthine were elevated, indicating the purine metabolism was enhanced in HFD-fed group. One possible explanation for this might be DNA damage and apoptotic cell death were caused by the increased reactive oxygen species resulting from excess dietary fat ²⁶. Hypoxanthine could be metabolized to xanthine by xanthine dehydrogenase or xanthine oxidase ²⁷. It has been considered that xanthine oxidase generated excess oxygen-free radicals, and then caused injury of islet cells in pathways ²⁷. After EPD and CA treated, the two metabolites were both decrease, indicating EPD and CA could regulate the purine metabolism. Meanwhile, xanthosine, a biomolecule for the synthesis of ATP, was elevated after EPD and CA treated ¹⁰. This might because these drugs could slow down the process of ATP synthesis, and thus causes an increase in the ratio of AMP/ATP. It has been reported the fluctuations in the AMP: ATP ratio could active AMP-activated protein kinase (AMPK), a major cellular energy sensor²⁸. Upon activation, AMPK could reverse the metabolic abnormalities associated with type 2 diabetes increases cellular energy levels by inhibiting anabolic energy consuming pathways (fatty acid synthesis, protein synthesis, etc.) and stimulating energy producing, catabolic pathways (fatty acid oxidation, glucose transport, etc.) ²⁹. Therefore, activation of AMPK might be contributed to the therapeutic effects of EPD and CA on T2DM.

It is worth noting that four biomarkers including tryptophan, N-Methyltryptamine, Glutathionylspermidine and Glutathion oxidized were reversed by EPD while these biomarkers were not significantly changed by CA. This might indicate EPD could regulate the tryptophan and glutathione metabolism while CA could not. Though CA is a main component of EPD, EPD contains many other triterpenoids such as ursolic acid, oleanolic acid, betulinic acid, euscaphic acid, pomolic acid and maslinic acid, all of which responsible for the therapeutic effects of EPD. Therefore, EPD could regulate more pathways than CA alone.

Conclusions

In this study, a metabolomic approach based on UPLC-Q-TOF-MS detection has been successfully established for biomarker exploration in T2DM and mechanism studies of EPD and CA. As a result, 26 metabolites were screened out and considered as potential biomarkers of T2DM. Taking these biomarkers as possible drug targets, it reveals EPD and CA could reverse the pathological process of T2DM through regulating the disturbed pathways of metabolism including purine metabolism, amino acid metabolism, tryptophan metabolism and lipid metabolism. Our findings revealed the potential effect of EPD and CA on these metabolic pathways and showed that provided a new methodological strategy for discovering the underlying efficacies and mechanisms of TCM.

Acknowledgements

This work was supported by the National Natural Science Foundation of China (No. 81102763 and 81373919) and the Natural Science Foundation of Jiangsu Province, (No. BK2011627). We also greatly appreciate the financial support from the Project Program of State Key Laboratory of Natural Medicines, China Pharmaceutical University (No. JKGQ201117) and the priority academic program development of Jiangsu higher education institutions (PAPD).

References

1. S. R. Barber, M. J. Davies, K. Khunti and L. J. Gray, *Diabetes research and clinical practice*, 2014.
2. P. Mirmira and C. Evans-Molina, *Translational research : the journal of laboratory and clinical medicine*, 2014.
3. C. S. Mizuno, A. G. Chittiboyina, T. W. Kurtz, H. A. Pershadsingh and M. A. Avery, *Curr Med Chem*, 2008, **15**, 61-74.

4. M. Tomczyk and K. P. Latte, *Journal of ethnopharmacology*, 2009, **122**, 184-204.
5. S. S. Wang, D. M. Wang, W. J. Pu and D. W. Li, *BMC complementary and alternative medicine*, 2013, **13**, 321.
6. J. Yang, H. Chen, L. Zhang, Q. Wang and M.-X. Lai, *Drug Development Research*, 2009, n/a-n/a.
7. L. Zhang, J. Yang, X. Q. Chen, K. Zan, X. D. Wen, H. Chen, Q. Wang and M. X. Lai, *Journal of ethnopharmacology*, 2010, **132**, 518-524.
8. C. Song, L. Huang, L. Rong, Z. Zhou, X. Peng, S. Yu and N. Fang, *Fitoterapia*, 2012, **83**, 1474-1483.
9. F. Du, A. Virtue, H. Wang and X. F. Yang, *Biomarker research*, 2013, **1**, 17.
10. G. Tan, W. Liao, X. Dong, G. Yang, Z. Zhu, W. Li, Y. Chai and Z. Lou, *PloS one*, 2012, **7**, e34157.
11. J. Yang, X. D. Wen, B. X. Jia, Q. Mao, Q. Wang and M. X. Lai, *Phytochemical analysis : PCA*, 2011, **22**, 547-554.
12. G. V. Dedoussis, A. C. Kaliora and D. B. Panagiotakos, *The review of diabetic studies : RDS*, 2007, **4**, 13-24.
13. J. J. Li, Y. Li, M. Bai, J. F. Tan, Q. Wang and J. Yang, *Biomedical chromatography : BMC*, 2014, **28**, 717-724.
14. S. J. Stohs, H. Miller and G. R. Kaats, *Phytotherapy research : PTR*, 2012, **26**, 317-324.
15. S. Takagi, T. Miura, E. Ishihara, T. Ishida and Y. Chinzei, *Biomedical research*, 2010, **31**, 213-218.
16. C. Zhu, Q. L. Liang, P. Hu, Y. M. Wang and G. A. Luo, *Talanta*, 2011, **85**, 1711-1720.
17. E. Schleicher and A. Nerlich, *Hormone and metabolic research*, 1996, **28**, 367-373.
18. R. G. Larkins and M. E. Dunlop, *Diabetologia*, 1992, **35**, 499-504.
19. S. H. Ayo, R. A. Radnik, W. F. Glass, 2nd, J. A. Garoni, E. R. Rampt, D. R. Appling and J. I. Kreisberg, *The American journal of physiology*, 1991, **260**, F185-191.
20. T. Huo, S. Cai, X. L. , Z. Xiong and F. Li, <http://www.paper.edu.cn>, 2008.
21. I. A. Leclercq, A. Da Silva Morais, B. Schroyen, N. Van Hul and A. Geerts, *Journal of hepatology*, 2007, **47**, 142-156.
22. D. Huang, J. Yang, X. Lu, Y. Deng, Z. Xiong and F. Li, *Journal of pharmaceutical and*

- biomedical analysis*, 2013, **76**, 200-206.
23. V. A. Ortega, D. A. Lovejoy and N. J. Bernier, *Frontiers in neuroscience*, 2013, **7**, 196.
24. K. H. Schulpis, E. D. Papakonstantinou and J. Tzamouranis, *Horm Res*, 2000, **53**, 32-35.
25. A. Stefanović, J. Kotur-Stevuljević, S. Spasić, N. Bogavac-Stanojević and N. Bujisić, *Diabetes research and clinical practice*, 2008, **79**, 156-163.
26. E. K. Daugherty, G. Balmus, A. Al Saei, E. S. Moore, D. A. Abdallah, A. B. Rogers, R. S. Weiss and K. J. Maurer, *Cell Cycle*, 2012, **11**, 1918-1928.
27. Y. H. Lv, X. R. Liu, S. K. Yan, X. Liang, Y. Yang, W. X. Dai and W. D. Zhang, *Journal of pharmaceutical and biomedical analysis*, 2010, **52**, 129-135.
28. S. Wang, P. Song and M. H. Zou, *Clinical science*, 2012, **122**, 555-573.
29. N. B. Ruderman, D. Carling, M. Prentki and J. M. Cacicedo, *The Journal of clinical investigation*, 2013, **123**, 2764-2772.

Figure 1 Experimental protocol for estimation of the therapeutical effects of EPD and CA on T2DM

Figure 2 EPD and CA ameliorated glucose intolerance in HFD treated mice.

After treatment with EPD and CA for seven weeks, the mice were fasted for 6h and orally administrated of glucose (2g/kg body weight). The levels of tail venous blood glucose in individual mice were measured at 0, 30, 60 and 120 min post glucose challenge. (A) Glucose concentrations within 2 h after glucose load. (B) Glucose AUC. The results were expressed as the mean \pm SD (n=6). *P<0.05 vs. HFD-fed group, #P<0.05 vs. normal group

Figure 3 Typical total ion chromatograms (TIC) of normal mice in (A) ESI⁺ mode and (B) ESI⁻ mode.

Figure 4 The PCA score plots of plasma samples collected from normal and HFD-fed groups in (A) positive and (B) negative ion modes.

Figure 5 The PLS score plots of plasma samples collected from normal and HFD-fed groups in (A) positive and (B) negative ion modes.

Figure 6 The S-plots derived from PLS. Each triangle in the loading plot represented an ion. (A) in positive and (B) in negative ion modes.

Figure 7 MS/MS spectra of xanthosine (the precursor ion was m/z 283.0673; the major fragment was m/z 151.0253); (A) Standard, (B) in plasma samples.

Figure 8 The PCA score plots of plasma samples collected from normal, HFD-fed, EPD and CA-treated groups in (A) positive and (B) negative ion modes.

Figure 9 Bar plots show UPLC -MS relative signal intensities for 26 metabolites in normal, HFD-fed, EPD and CA-treated groups. Data are expressed as mean \pm S.D.

Figure 10 The network of the potential biomarkers changing for HFD-fed, EPD and CA-treated modulation according to the KEGG PATHWAY database.

*p<0.05 vs. HFD-fed group, #p<0.05 vs. normal group

Table 1 Effects of EPD and CA on blood biochemical characteristics.

	Normal	HFD-fed	CA-treated	EPD- treated
Body weight(g)	28.92±2.01	42.12±2.17 [#]	34.22±1.98*	32.18±1.42*
TG(mg/dL)	72.13±10.56	132.04±10.13 [#]	87.33±4.56*	85.27±11.39*
TC(mg/dL)	89.24±6.37	249.32±10.14 [#]	101.27±6.42*	119.59±4.78*
LDL-c(mmol/L)	0.88±0.14	2.95±0.24 [#]	1.28±0.18*	1.16±0.14*
HDL-c(mmol/L)	1.92±0.16	1.00±0.15 [#]	1.72±0.14*	1.82±0.20*
FBG (mmoL/L)	4.08±0.92	8.21±1.22 [#]	4.58±0.44*	4.99±0.67*
Fins (mIU/L)	24.37±10.92	126.83±42.32 [#]	25.92±9.72*	25.47±6.82*
HOMA-IR	4.41±2.19	46.27±21.82 [#]	5.28±2.91*	5.65±3.52*

*P<0.05 vs. HFD-fed group, [#]P<0.05 vs. normal group

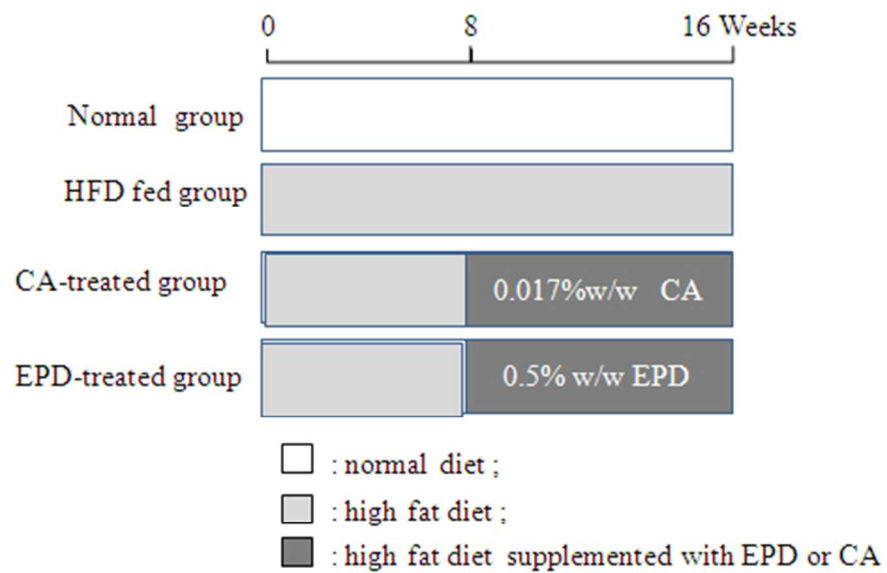


Figure 1 Experimental protocol for estimation of the therapeutical effects of EPD and CA on T2DM
141x88mm (96 x 96 DPI)

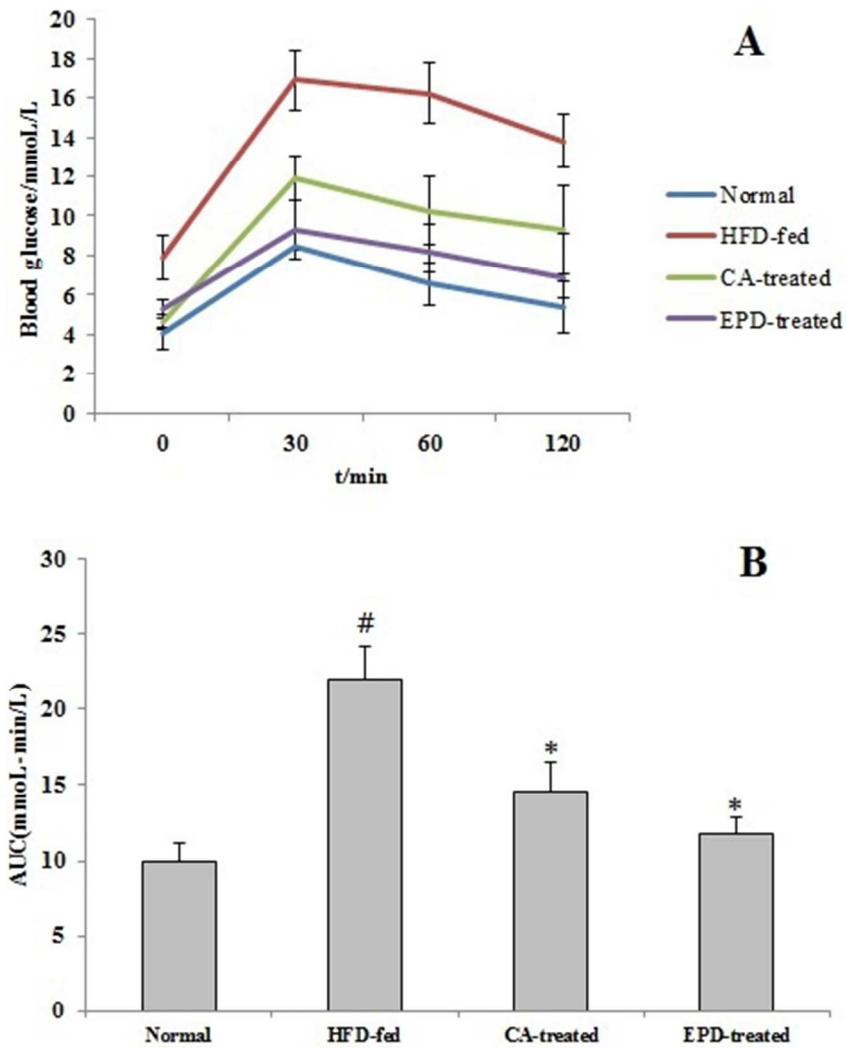


Figure 2 EPD and CA ameliorated glucose intolerance in HFD treated mice.
96x111mm (144 x 144 DPI)

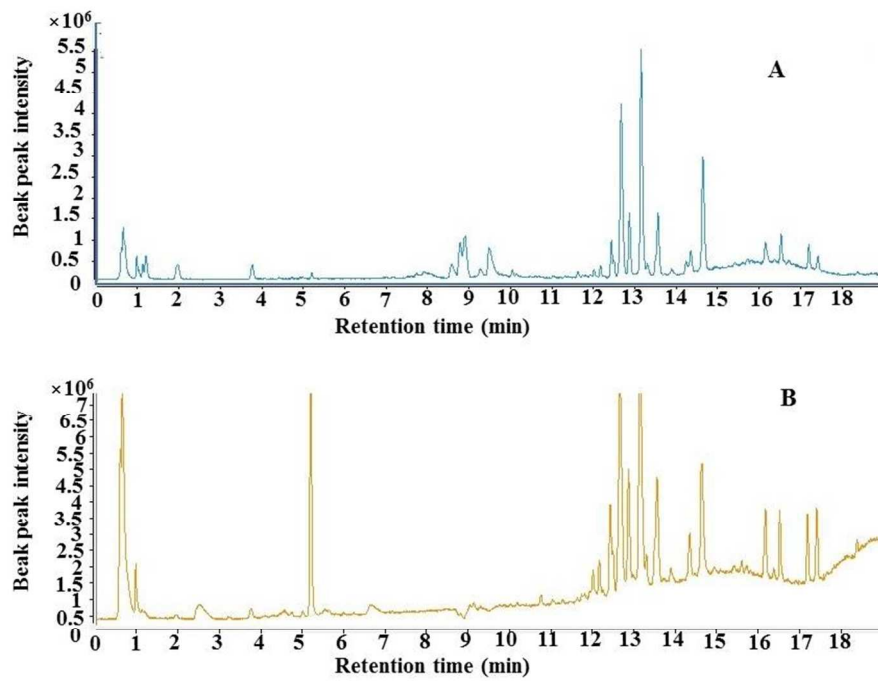


Figure 3 Typical total ion chromatograms (TIC) of normal mice in (A) ESI+ mode and (B) ESI- mode.
254x190mm (96 x 96 DPI)

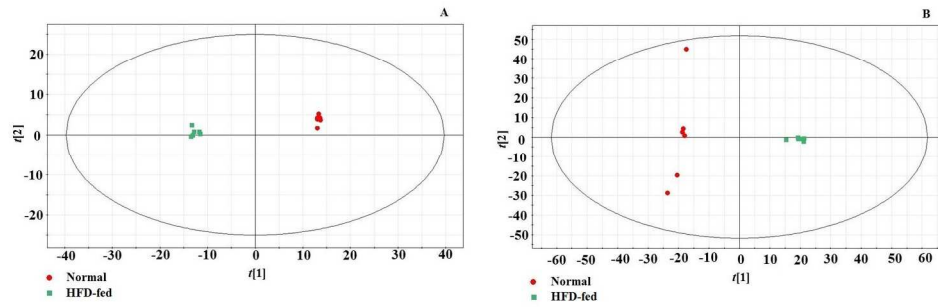


Figure 4 The PCA score plots of plasma samples collected from normal and HFD-fed groups in (A) positive and (B) negative ion modes.
343x130mm (144 x 144 DPI)

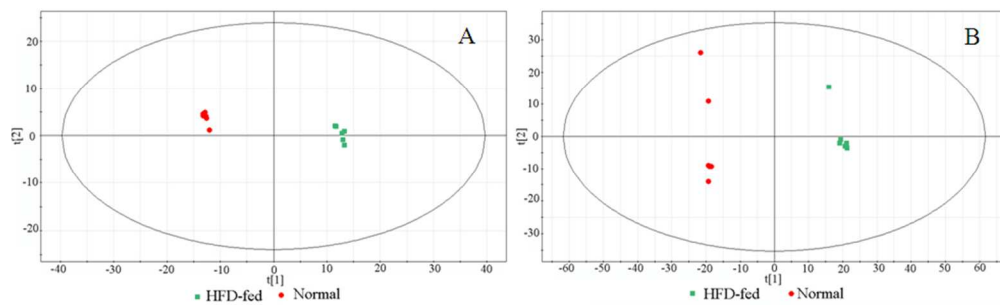


Figure 5 The PLS score plots of plasma samples collected from normal and HFD-fed groups in (A) positive and (B) negative ion modes.
260x88mm (96 x 96 DPI)

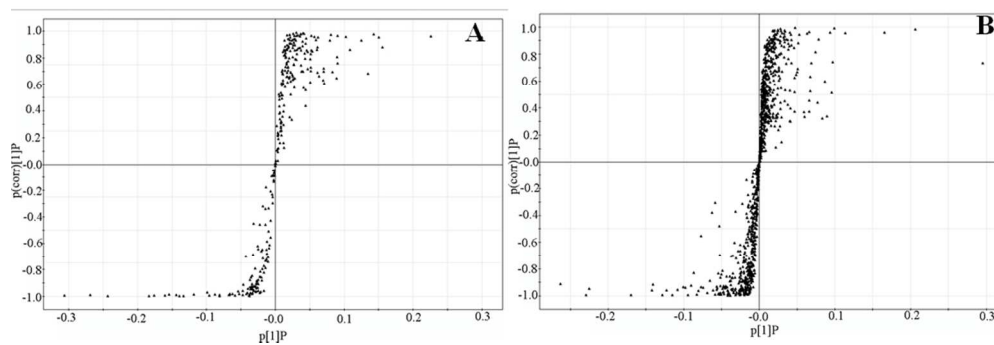


Figure 6 The S-plots derived from PLS. Each triangle in the loading plot represented an ion.
302x103mm (96 x 96 DPI)

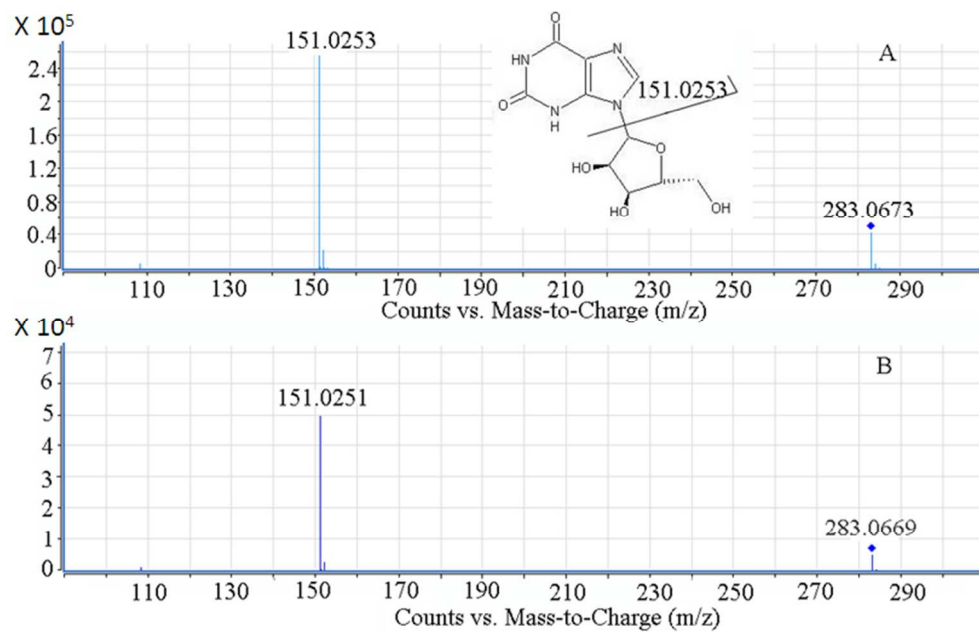


Figure 7 MS/MS spectra of xanthosine (the precursor ion was m/z 283.0673; the major fragment was m/z 151.0253)(A) Standard, (B) in plasma samples
219x138mm (96 x 96 DPI)

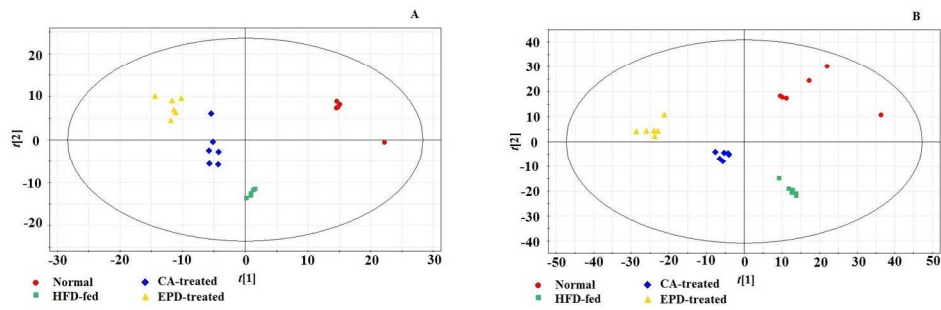


Figure 8 The PCA score plots of plasma samples collected from normal, HFD-fed, EPD and CA-treated groups in (A) positive and (B) negative ion modes.
343x130mm (144 x 144 DPI)

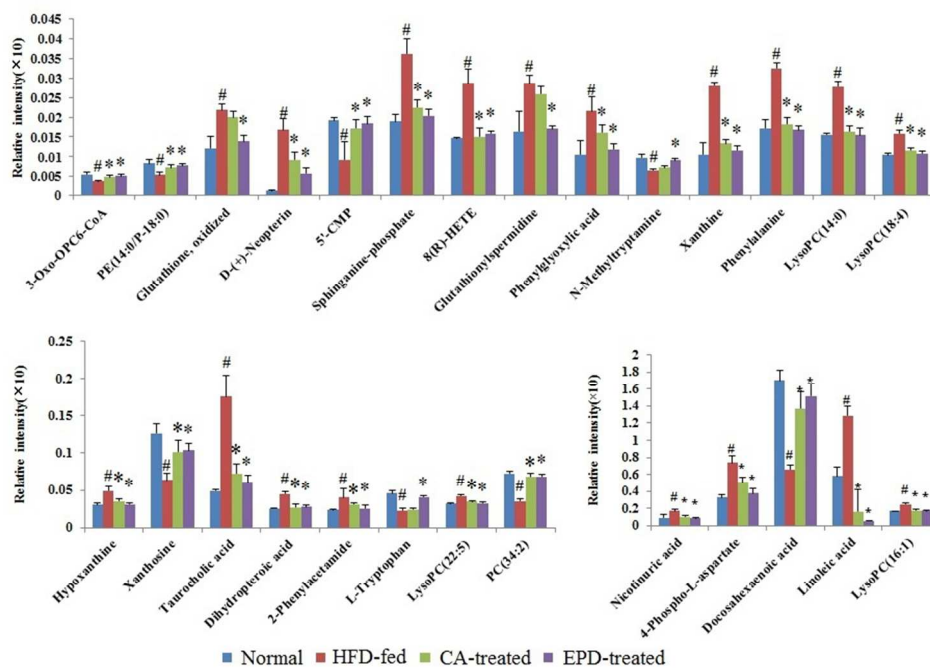


Figure 9 Bar plots show UPLC -MS relative signal intensities for 26 metabolites in normal, HFD-fed, EPD and CA-treated groups.
170x118mm (144 x 144 DPI)

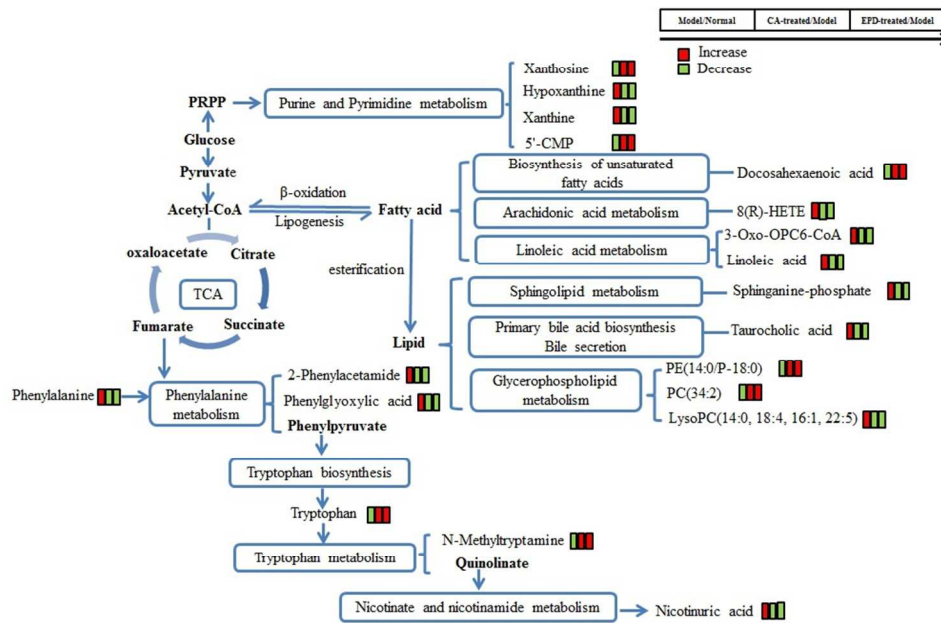


Figure 10 The network of the potential biomarkers changing for HFD-fed, EPD and CA-treated modulation according to the KEGG PATHWAY database.
185x126mm (144 x 144 DPI)